Australian Journal of Basic and Applied Sciences, 6(13): 536-557, 2012
ISSN 1991-8178

Lithofacies, Diagenesis and Geochemical Analysis of the Lower Cretaceous Risan Aneiza Formation at Gabal Manzour, North Sinai, Egypt.

F.S. Ramadan and Samir M. Zaid

Geology Department, Faculty of Sciences, Zagazig University, 44511 Zagazig, Egypt

Abstract: The Lower Cretaceous (Aptian- Albian) rocks exposed in Gabal Manzour, north Sinai Peninsula are described and interpreted on the basis of field observations, facies and geochemical analyses to give information on their depositional environments, diagenetic sequence and geochemical characteristics. Depend on their lithologic characteristics, the Aptian- Albian succession consists of mixed siliciclastic–carbonate rocks. This succession is dominated by carbonate production in the northern and eastern parts of the study area. Detailed petrographic investigations recognized twenty clastic and carbonate facies types. These facies and their related palaeoenvironments indicate transition from interior ramp environments (i.e., lagoon, backshoal, and shoal); intertidal and low-energy subtidal facies interfingers with a few storm-influenced deposits. The main factors controlling facies deposition were eustatic sea-level fluctuations combined with environmental influences such as autochthonous carbonate productivity and siliciclastic supply. Diagenetic processes have greatly affected limestones and sandstones of Risan Aneiza Formation. The diagenetic sequence, for limestones include: micritic envelopes, dissolution of aragonite, cementation, compaction, and dolomitization, while the major diagenetic aspects observed in Risan Aneiza sandstones are: compaction, silica overgrowth, carbonate cementation, mixture of clay and iron oxides filling, iron oxides cementation and evaporite cementation. Geochemical study revealed that there are highly positive correlations between Cr, Ni, Rb and Pb and between Sr, Ba and Pb, and a highly negative correlation between Cr, Co and Cu, which reflect their derivation from mixed carbonate- siliciclastic sources. Also, there is no correlation between uranium and any other trace elements, which indicates that these elements that leached by modern meteoric water from nearby outcrops of Miocene and younger marine strata, transported in surface and ground water to the topographically low terrain where the Aptian- Albian rocks crop out.

Key words: Diagenesis, Geochemical analysis, Gabal Manzour, Lower Cretaceous, Sinai, Egypt

INTRODUCTION

The present work is devoted to study the Lower Cretaceous Risan Aneiza Formation in Gabal Manzour. It is located on the northeastern flank of Gabal Maghara anticline. It lies in the northeastern part of Sinai Peninsula at Latitudes 30° 40\ to 30° 59\ N and Longitudes 33° 23′ to 33° 35′ E (Fig.1). It is located on the northeastern flank of Gabal Maghara anticline.

Despite the fact that the Sinai region has received much attention by many eminent geologists since the beginning of the last century, only few works focused on Gabal Manzour. Numerous studies have been published on the geology, stratigraphy, and paleontology of the Lower Cretaceous exposed in the north Sinai such as Aly (1988), Philip *et al* (1988), Hegab *et al*. (1989), Aboul Ela *et al* (1991), Ibrahium (1992), Hassaan *et al*. (1992), El Sheikh and Aly (1994) , Hamza et al (1994),El-Araby (1999), Hewaidy and Morsi (2001), Bachmann et al (2003), El -Azabi and El Araby (2005), Abu Zied (2007), Wanas (2008) and Hamama (2010) and others.

The present work focuses on the facies analysis, diagenesis, geochemistry and depositional environments of the Lower Cretaceous sedimentary rocks cropping out in north Sinai at Gabal Manzour. This approach makes it possible to follow the facies analysis, diagenetic aspects and to establish a depositional environment for the Lower Cretaceous strata in north Sinai. To achieve this work, a composite stratigraphic section of Lower Cretaceous rocks were measured, described and sampled. The indurated rocks were thin-sectioned and investigated under the polarized microscope to illustrate and describe the microfacies types. The limestone and sandstone microfacies were described following the classifications of Carozzi (1960) and Pettijohn (1975).As well as, eleven trace elements (Cr, Mn, Co, Ni, Cu, Zn, Pb, Rb, Ba, Sr and U) have been qualitatively determined in 19 bulk samples representing the various facies to delineate relationship between the facies setting, the physicochemical features of the sedimentation, and the subsequent processes of diagenesis.

2. Tectonic Setting:

Corresponding Author: F.S. Ramadan, Geology Department, Faculty of Sciences, Zagazig University, 44511 Zagazig, Egypt

Sinai Peninsula is bounded by major tectonic elements. These are the Mesozoic-Early Cenozoic tectonically-active Tethys Sea to the north, the Oligo-Miocene Gulf of Suez rifted basin to the west, and the late Miocene to Recent transform Dead Sea-Gulf of Aqaba rift to the east. Each of these major elements has affected dramatically the structure and tectonic evolution of the north Sinai area.

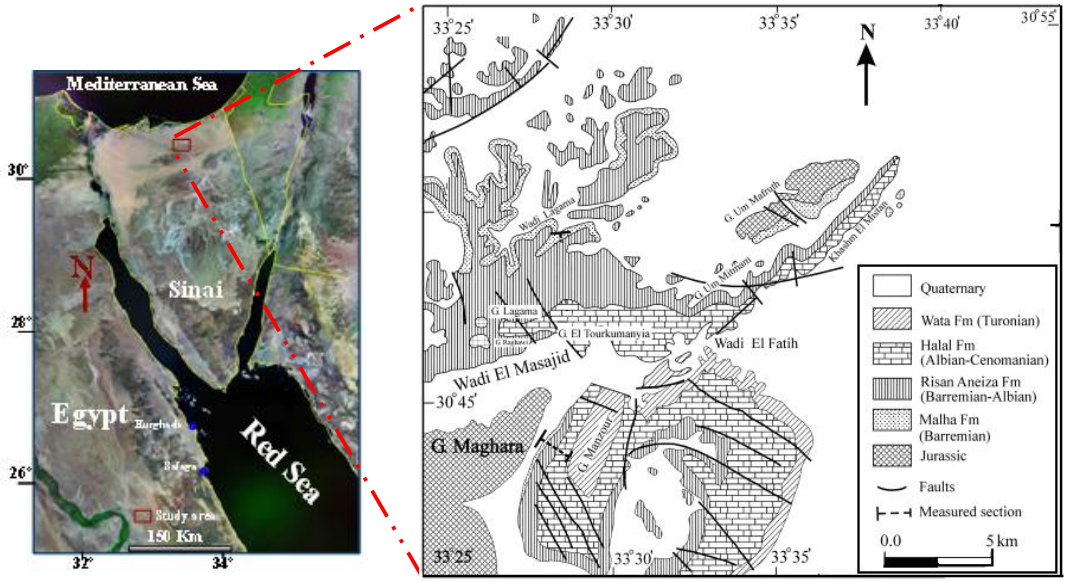

Fig. 1: Geological map of the study area, modified after the Geological Survey of Egypt, (1992).

In Late Triassic time, the breakup of north Africa-Arabia and the opening of the Tethys took place and reactivated ENE-WSW-oriented deep-seated faults (Fig. 1). The southern and central sectors of Sinai were uplifted, relative to the northern one (onshore and offshore); Bartov *et al*., 1980. The influence resulted in the development of a thick wedge of the Early and Middle Mesozoic sediments (Triassic, Jurassic and Early Cretaceous) in the northern sector and its abrupt thinning to the south. Structurally, this phase was dominated by Jurassic NW-SE left-lateral oblique extension which resulted in ENE- to NE-trending normal faulting (Aal and Lelek, 1994). In the Early Cretaceous times, The Sinai Peninsula was a part of broad shallow shelf situated on the southern passive margin of the Neo-Tethys, where a carbonate platform with siliciclastic intercalations was established (Kuss and Bachmann, 1996 and Bauer *et al*., 2001).

During the Late Cretaceous to Early Tertiary (Laramide) time, Africa moved west-northwest relative to Eurasia, which closed the Tethys Sea and produced a right-lateral shear couple between North Africa and Eurasia (Smith, 1971). This shear couple started in the Turonian, climaxed in the Late Cretaceous and decreased into the Early Tertiary, causing the right-lateral rejuvenation of the deep-seated faults in north Egypt (Smith, 1971). This tectonic event, known in the Middle East as Syrian arc system, produced a series of asymmetrical NE-trending, doubly-plunging anticlines in the study area, e.g., Gabal Maghara (Fig. 1). Therefore the study area is believed to have remained tectonically rather quiet throughout Early Cretaceous (Kuss and Bachmann, 1996). The sedimentary successions in North Sinai were deposited in half graben sedimentary basins during the Early Mesozoic and were later inverted and folded during Early Cretaceous as a result of the Laramide compressive movements (Ayyad *et al*., 1998). Structural studies across north Sinai indicated syndepositional tectonism revealed by the abrupt thickening of Jurassic strata northward.

3. Lithostratigraphy:

The Lower Cretaceous rocks in north Sinai, have extensively been studied stratigraphically and paleontologically by several authors such as Aly (1988), Ibrahium (1992), El Sheikh and Aly (1994) and Issawi *et al*. (1999), Hewaidy and Morsi (2001), Bachmann *et al* (2003), El -Azabi and El Araby (2005), Abu Zied (2007), Wanas (2008) and Hamama (2010) and others. The Jurassic rocks were considered the oldest rocks exposed in the study area (Hassaan *et al*., 1990). These rocks are overlain by the Lower and Upper Cretaceous terrigneous carbonate rocks (Fig. 1).

In north Sinai, the Risan Aneiza Formation is assigned an Aptian-Early Albian age (Said, 1971 and Hamza *et al*. 1994). The Risan Aneiza Formation was firstly described at Gebel Lagama, north of Gebel El-Maghara, northern Sinai (Fig. 1), and is about 110 m thick.

In the studied section, the Risan Aneiza Formation unconformably overlies the Malha Formation (Barremian) and conformably underlies the Halal Formation (Cenomanian). It includes 68 recognizable units consisting mainly of sequences of green shale, limestone and marl beds with interbedded sandstones recording a maximum thickness of about 234.75m. These marl beds are very rich in *orbitolines* and megafossils (Fig. 2). The typical Aptian- Albian rocks appears as yellowish olive –coloured, oolitic, orbitolinoid- rich dolomitic limestones that lies directly below the Cenomanian *Exogyra* rich marl which overlaying Halal Formation. Risan Aneiza Formation can be differentiated into two members based on field observation, lithologic characteristics, microfacies types, fossils content and sedimentary structures (Fig. 2). The following is a brief description of the two members.

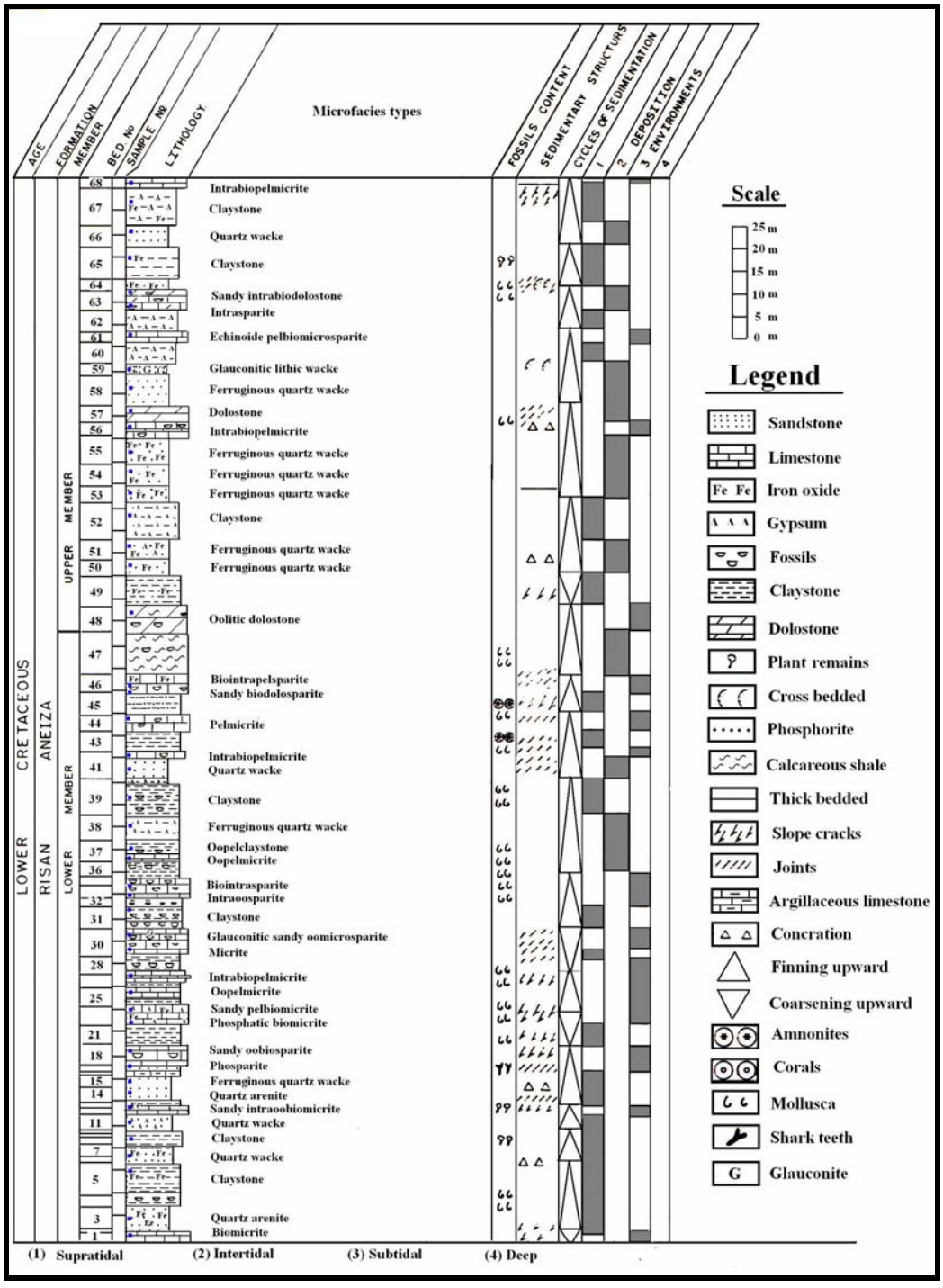

Fig. 2: Stratigraphic column, microfacies analysis and depositional environments of studied section of Gabal Manzour area, Sinai.

3.1. Lower Member:

It can tentatively be subdivided into two parts:

The lower part is dominated by sandstone and claystone beds. Sandstones are yellowish red, moderately hard with gypsum veinlets in some parts, while claystones are grayish, dark reddish brown, cracked, saliferous and contain a few badly preserved *pelecypods* with some scattered silicified plant remains. The few carbonate interbeds are composed of limestone. The upper part is mainly composed of limestones, marls and claystones. The limestones are yellowish orange and highly fossiliferous. The limestones display an oolitic nature at the base of this part, however, the marl and claystone beds display yellow to olive color and they are moderately hard, saliferous, and gypsiferous and contain Mn-oxide patches. The faunal assemblage, that includes; *pelecypods-gastropods, exogyra, oysters, ammonites, corals and echinoids*, as well as shell fragments and shark teeth. The contact between the two parts is characterized by the presence of moderately hard phosphatic band, forming a ledge and capped by badly preserved fossiliferous marl beds.

3.2. Upper Member:

It could be differentiated into two parts:

The lower part is composed of clastic facies (sandstones and claystones). It is conformable with respect to the underlying rock unit. This part of the section is barren of fossils. The claystone beds are light gray, compact, ferruginous and intercalated by gypsum bands. The upper part is made up of limestone, dolostone, sandstone and claystone beds. They are very hard, dissected and sporadically contain manganiferrous materials. The sandstones are fine to very fine- grained, slightly hard, ferruginous, concretionary, jointed and cracked. Going upward they becoming bedded and cross- bedded forming a ridge. The claystones display brownish hues due to ferrugination. They contain gypsiferous streaks and enriched in plant remains. The contact between the two members is easily distinguished by oolitic highly ferruginous dolostone beds.

4. Microfacies and Depositional Environment:

The microfacies study is based on petrographic examination of 100 thin sections, representing the different lithologies of the Risan Aneiza Formation. Twenty sedimentary facies of both carbonate and clastic rocks are recognized in the studied Aptian – Albian rocks. The study revealed six microfacies (micrite, microsparite, sparite, dolomite, sandstone (quartz wacke, glauconitic wacke and quartz arenite) and claystone) with twenty submicrofacies. These facies show four depositional environments (peritidal, lagoon, high energy shoals of ooids, and intertidal – subtidal marine environments). The following is a brief description of the different facies recognized through the studied section:

4.1 Micrite Microfacies:

This facies is well recorded in both lower and upper members at the studied section (Fig. 2). It is mainly made up of mud and supported grains range from 5-25%. The micrite beds fluctuate in thickness between 0.5- 3 m with variable proportions of allochems. Fossils, pellets, ooids and intraclasts are abundant as well as non-carbonate particles represented by quartz, glauconite and phosphate grains. The rocks of this microfacies can be divided into five submicrofacies, as follows;

4.1.1 Biomicrite:

The rocks of this submicrofacies are grayish white, massive and hard. It is build up of molluscan shell fragments, benthonic and planktonic foraminifera (40%), *echinoid* plates (15%), *milliloids (10%)*, *annelid* tubes (10%) and few scattered peloids (5%) embedded in micrite matrix (Plate 1, Fig.1). Most skeletal grains and foraminiferal tests are completely replaced by or filled with sparry calcite. Few rounded to subrounded quartz grains are scattered throughout the rock.

***Interpretation*:**

The high diversity of organisms, presence of large bioclasts, echinoids, and abundance of molluscan shell fragments and benthonic foraminifera in micrite matrix, suggest deposition in a subtidal environment with open circulation (Wilson, 1975; Flügel, 1982 and Harris *et al*., 1997).

4.1.2 Pel-biomicrite:

The rocks of this submicrofacies are dusty yellow, hard, compact, argillaceous, and intercalated with gypsum bands. Microscopically, it consists of shell fragments (25%), benthonic foraminifera (15%), *echinoid* plates and spines (15%) and peloids (25%) embedded in micrite matrix. Peloids are subcircular to circular,

sorted and composed of micritized grains (Plate 1, Fig. 2). Few scattered quartz grains medium to fine, subangular to angular and mostly have undulose extinction are recorded.

***Interpretation*:**

The thin bedded, abundant lime mud and peloids and diverse lagoonal type biota, typically indicate restricted subtidal quiet water, probably a restricted lagoon or sheltered bays (Hottinger, 1997; Pittet *et al*., 1995).

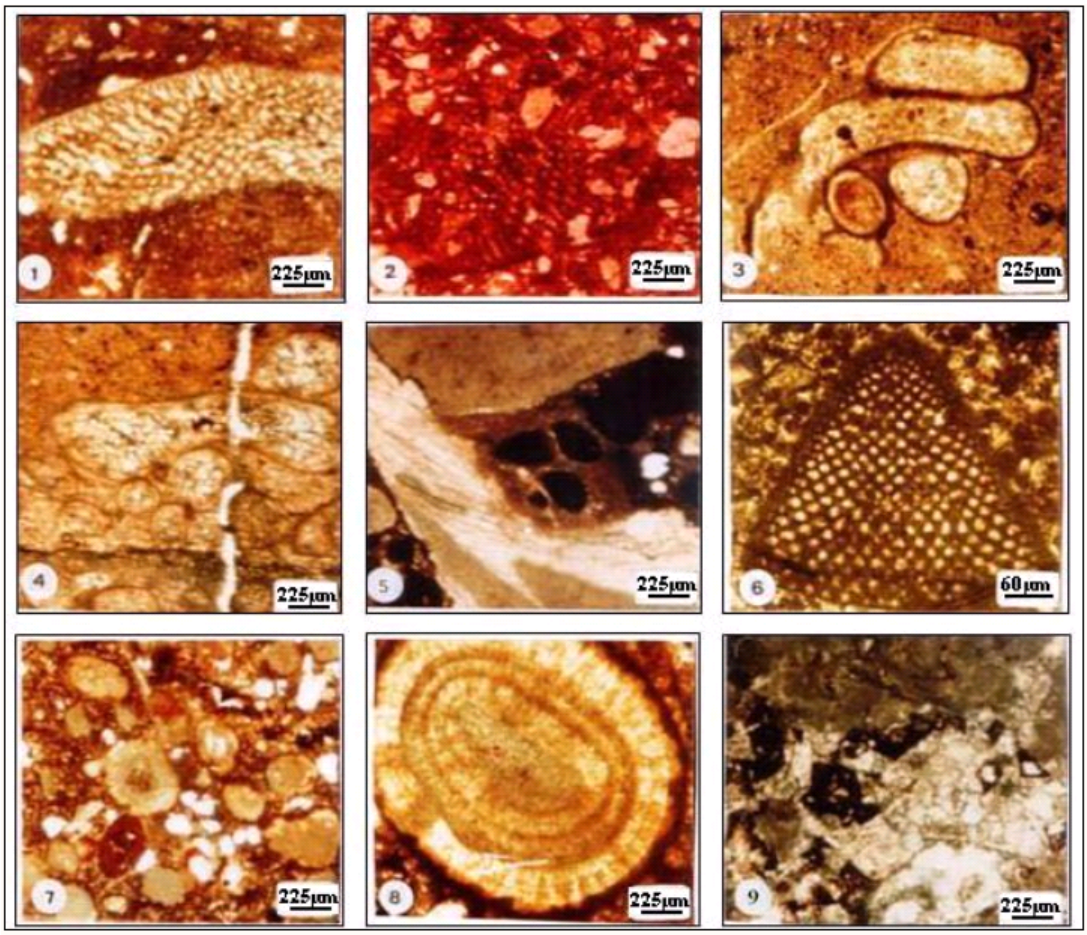

Plate 1: Photomicrograph showing; **1:** Biomicrite, foraminifera *(Orbitilina* sp) and a few scattered peloids and quartz grains are embedded in micrite matrix. PPL, Bed No.1, **2:** Sandy pel-biomicrite, shell fragments, echinoid spines and small peloids embedded in micrite matrix. C.N, Bed No. 24, **3:** Oo-pelmicrite, regenerated and broken ooids in the micritic matrix. PPL, Bed No.25, **4:** Tangential structure, characterized by light colour lamellae, oriented sparry calcite cement. Note, fracture to cut off the components. PPL, Bed No. 25, **5:** Phosphatic biomicrite, molluscan shell fragments and collophane grains embedded in micrite matrix. Partially shell fragments recrystallized to sparry calcite. C.N, Bed No. 23, **6:** *Orbitilina* sp with peloidal grains in micritic matrix. C.N, Bed No, 27, **7:** Several ooids, single or multiple layers, concentric and some radial fibers internal structure. Also, scattered glauconite grains are recorded. C.N, Bed No. 30**, 8:** Close up of ooids; concentric internal structure. C.N, Bed No. 30, **9:** Dolomite rhombs rimed and stained by iron oxides (Ferroan type) represented in microsparite cement. PPL, Bed No.57.

4.1.3 Oo-pelmicrite:

The rocks of this submicrofacies are massive grayish yellow to yellowish brown. It is composed of 40-50% peloids, 20-25% ooids, and few echinoid plates 5-10% with binding material of micritic matrix. Peloids are rounded, poorly sorted and composed of micritized grains. Ooids are of normal type with few cortices and

spherical to ovular shapes (Plate 1, Figs. 3 and 4). Some ooids are half-moon and cracked type due to stress and pressure solution.

***Interpretation*:**

The occurrence of ooids and abraded shells indicates deposition under agitated conditions above the fair – weather wave base (intertidal zone); Dunham, 1962. Therefore, co-existence of ooids, peloids and low bioclasts embedded in lime mud may be proposed to deposit in a lower intertidal environment (Flugel, 1982).

4.1.4 Phosphatic biomicrite:

The rocks of this submicrofacies are grayish yellow, hard, compact, massive, argillaceous and interbedded with gypsum bands. It consists of fossil and shell fragments (40-50%), phosphate grains (20-30%), few glauconite pellets (3%) and rare intraclasts (2%) embedded in micritic matrix. The most of bioclastics (*Orbitilina* sp. and *echinoid* plates) are recrystallized and few others are preserved with original texture. The phosphate clasts are made of collophane pellets and/ or scattered bone fragments (Plate 1, Fig. 5). They range in size from coarse to fine sand size and irregular in shape.

***Interpretation*:**

The abundant lime mud and diverse lagoonal type biota typically indicates restricted subtidal quiet water, probably a restricted lagoon or sheltered bays (Hottinger, 1997; Pittet *et al*., 1995). The occurrence of phosphate grains, glauconite pellets and rare intraclasts in the micrite matrix support the deposition in a protected quiet water zone (Tucker and Wright, 1990).

4.1.5 Intra-biopelmicrite:

The rocks of this submicrofacies are grayish orange to yellowish brown, moderately hard, fossiliferous, ferruginous, clayey upwards and nodules forming some parts. It consists of peloids (30-40%), orbitinoid foraminiferal shell fragments (10-20%), echinoid plates (10-15%) and intraclasts (10-15%) embedded in micritic matrix. Peloid grains are well rounded, subspherical to spherical, partially filled by sprite. They are composed of micrite or rimed by micrite envelope. The shell fragments are composed essentially of *mollusca, echinoid, bryozoa and Orbitilina* foraminifera (Plate 1, Fig. 6). Most fossil fragments and foraminiferal tests are filled by sparite and occasionally stained by ferruginous materials. The intraclasts occur in coarse to medium sand size grained, and are composed of micrite or quartz grains, fossils fragments and pellets.

***Interpretation*:**

The occurrence of intraclasts within the bio-pelmicrite facies suggests reworking from the nearby carbonate shoals to the shallow subtidal water where the micrite forming matrix is deposited. This can takes place during storm influence on deposition in the shallow subtidal zone (Lee and Kim, 1992). In addition, nodular nature of the characteristic limestones may refer and support an occasional period of storm activity (Bàdenas and Aurell, 2001).

4.2 Microsparite Microfacies:

This facies describes sediments containing matrix of heterogeneous dark micrite and /or coarse microsparite. It is recorded in both lower and upper members at the studied section (Fig. 2). The microsparite beds fluctuate in thickness between 1.5- 5 m with variable proportions of allochems. The micrite matrix may exists side by side with microsparite, forming clotted fabric. This microfacies can be subdivided into three submicrofacies, as follows;

4.2.1 Glauconitic sandy oomicrosparite:

The rocks of this submicrofacies are grayish orange, hard, laminated in the base and thin bedded upwards. It contains abundant ooids (40-50%), quartz grains (10-15%) and glauconite (10%) besides few bioclasts and intraclasts (5%), embedded in microsparite matrix (Plate 1, Fig.7). The ooids display proper concentric structure with inferred radial structure. They are oval to elongated in shape, and contain nuclei either of bioclasts or micritic fragments. They are partially recrystallized to sparite (Plate 1, Fig. 8). Glauconite grains are reddish, slightly weathered and rounded to subround. Quartz grains occur in the medium to fine sand size, subrounded and moderately sorted.

***Interpretation*:**

Ooids with concentric structures and ooid aggregates indicate deposition in an intertidal zone of highly agitated shallow water conditions (Strasser, 1986). In addition, the presence of intraclasts, terrigneous quartz

grains and low organism diversity, refer and support an intertidal zone environment (Flugel, 1982). Therefore, the recognized oolitic microsparite refers to deposition in a high-energy intertidal shoal.

4.2.2 Dolomicrosparite:

The rocks of this submicrofacies are yellowish brown, hard, and low fossiliferous. The microsparite matrix is markedly dolomitized. Dolomite is zoned, stained and idio-to hypidotopic texture. Ferroan dolomite occurs as a source of the late diagenetic stage (Plate 1, Fig. 9). A few sparite patches and micrite material set in microsparite matrix are due to recrystallization process.

***Interpretation*:**

The fine crystalline dolomites have been interpreted to be a result of penecontempraneous dolomitization of precursor micrite in supratidal flat sediments during regressive phase in upper intertidal to supratidal setting (Warren, 2000). The recognized fine crystalline dolomites with rare evaporites are in a close similarity with the dolostones of upper intertidal– supratidal zone in platform carbonate that were formed during sea-level fall (Qing *et al*., 2001; Abu El-Hassan and Wanas, 2005).

4.2.3 Echinoid pel-biomicrosparite:

The rocks of this submicrofacies are grayish orange, hard, massive, with ferruginous band in its lower part. It is composed of shell fragments (30-40%), foraminifera (15-20%), peloids (10-20%) and echinoids (7-10%) with few dolomite crystals (3%) embedded in microsparite groundmass. Molluscan shell fragments, echinoids are ill preserved, disoriented and partially recrystallized (Plate 2, Fig. 1). The foraminifera are sometimes enveloped by micrite rims. Peloids are fine grained, rounded, moderately sorted and consist of micritic materials. Cements seem to have been by gypsiferous material at an early stage, followed by ferrugination.

***Interpretation*:**

This facies is characterized by: 1) the high diversity of organisms, planktonics are abundant and benthonics are rare); 2) the abundant bioclasts are large to very large size; and 3) abundance of molluscan shell fragments, embedded in micrite matrix. These suggest deposition in a deep subtidal environment (Wilson, 1975; Flügel, 1982 and Harris *et al*., 1997).

4.3 Sparite Microfacies:

This facies is well recorded in both lower and upper members at the studied section (Fig. 2). The sparite beds fluctuate in thickness between 0.5- 4.5 m with variable proportions of allochems. The carbonate particles are dominant and represented by skeletal grains, peloids, ooids aggregate, intraclastics and minor detrital and few quartz. This microfacies is subdivided into five submicrofacies, as follows:

4.3.1 Intra -oosparite:

The rocks of this submicrofacies are yellowish orange, hard, compact, and ferruginous. It is made up of ooids (40-50%), intraclasts (15-20%) with few quartz grains (3%) and glauconite pellets (2%) embedded in sparry calcite cement. Ooids are varying in size, asymmetrical; most of them are single type, while others are a composite type. Some ooids are half moon deformed, cracked, truncated or stained by ferruginous material. Intraclasts are subrounded, moderately sorted and composed of micritic materials, bioclasts fragments and ferruginous materials. Siliceous and ferruginous thin deformation cracks are observed (Plate 2, Figs. 2 and 3).

***Interpretation*:**

The occurrence of ooids and abraded shells in sparry calcite cement indicates deposition under agitated conditions above the fair-weather wave base (Dunham, 1962; Strasser, 1986). On the other hand, the presence of intraclasts, terrigneous quartz grains and low organism diversity, refers to deposition in a high-energy intertidal shoal (Flugel, 1982).

4.3.2 Bio -intrapelsparite:

The rocks of this submicrofacies are yellowish brown, hard, bedded, and ferruginous. It consists of peloids (30-40%), intraclasts (20-30%), and fossils fragments (10-15%) embedded in sparry calcite cement. The peloids are spherical to elliptical in shape, well rounded, moderately sorted and composed of micrite and partially stained by iron hydroxides. Intraclasts have complex structure, and composed of broken micrite particles, bioclasts, ooids and opaque grains. Bioclasts (*bryozoa, pelceypods* and *gastropods*) are partially replaced by either fibrous calcite or ferruginous materials (Plate 2, Figs 4 and 5).

***Interpretation*:**

The low diversity of shell fragments and the occurrence of intraclasts within the pelsparite facies suggest reworking from the nearby carbonate shoals to the shallow subtidal water where sparry calcite is formed (Wilson, 1975 and Flügel, 1982). This can take place during storm influence on deposition in the shallow subtidal zone (Lee and Kim, 1992). In addition, nodular nature of the characteristic limestones may refer and support an occasional period of storm activity (Bàdenas and Aurell, 2001).

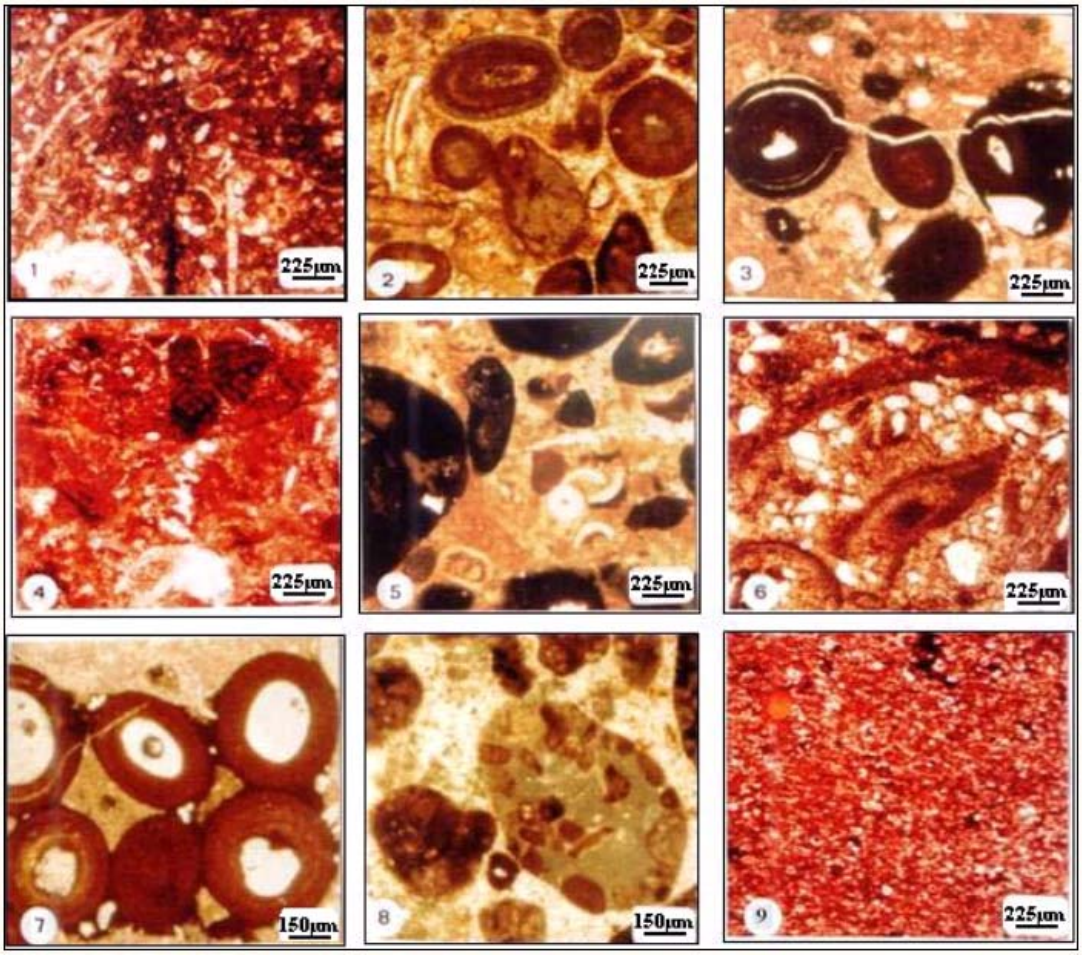

Plate 2: Photomicrograph showing; **1:** Echinoid pel-biomicrosparite; echinoid spine with few shell fragments set in microsparite cement. C.N, Bed No. 61, **2:** Intra -oosparite; intraclastics with ooids embedded in sparry calcite cement. Note, intraclasts consists of bioclastic fragments. C.N, Bed No.33, **3:** The internal structure of ooids is commonly dissolved, sometimes nuclei of ooids may be preserved and the crust of ooids are composed of dark micritic material admixed with iron oxides. PPL, Bed No. 33, **4:** Bio intra pelsparite; most intraclasts are stained and rimed with iron oxides. C.N, Bed No. 46, **5:** Bio-intrasparite; intraclastics and echinoid spine are embedded in sparry calcite cement. PPL, Bed No. 46, **6:** Sandy bio-dolosparite facies is partially dolomitized the molluscan fragments , medium to coarse quartz grains embedded in sparry calcite cement. C.N, Bed No. 46, **7:** Various nuclei ooids; quartz nuclei, micritic nuclei and sparite nuclei. Note, they appear as closing layer and notice blanking. C.N, Bed No. 32, **8:** Complex intrasparite structure, various in sizesand fine quartz grains embedded in sparry calcite cement. C.N, Bed No. 63, **9:** Very fine dolomite rhombs showing cloudy centers and most dolomite rhombs rimed with iron oxides. C.N, Bed No. 57.

4.3.3 Sandy bio-dolosparite:

The rocks of this submicrofacies are grayish orange, hard, massive, fossiliferous and dolomitic. It is made of dolomite crystals (20-30%), echinoids (20-30%), fossil fragments (15-20%) and quartz grains (10%) embedded in sparry calcite cement. Echinoid plates and mollusca shell fragments are ill sorted, medium sand

sized, bladed in shape and partially recrystallized. Quartz grains are medium to coarse, subrounded, and moderately sorted. Dolomite rhombs are ooze size, cloudy centers, xenotopic texture and shown one phase of dolomitization. Most components are stained and rimed with iron oxides (Plate 2, Fig.6).

***Interpretation*:**

The high diversity of organisms, presence of echinoids, terrigeneous sand grains and abundance of molluscan shell fragments in sparry calcite cement suggest deposition in intertidal - shallow subtidal environment with open circulation (Wilson, 1975; Flügel, 1982 and Harris *et al*., 1997).

4.3.4 Sandy intra-oosparite:

The rocks of this submicrofacies are yellowish brown, hard, cross bedded and phosphatic. It is composed of ooids (40-50%), intraclasts (15-20%) and quartz grains (10-20%) embedded in sparry calcite cement. Ooids are coarse sized, spherical, well sorted, and most of them have nuclei. The ooids microstructure is concentric and stained with iron oxides. Quartz grains occur in nuclei of most ooids and as scattered grains. The former is coarse grained, monocrystalline and rounded while the latter is fine grained subangular and polycrystalline grained (Plate 2, Fig. 7).

***Interpretation*:**

In general, ooids with concentric structures and ooid aggregates indicate deposition in an intertidal zone of highly agitated shallow water conditions (Wilson, 1975; Strasser, 1986; Harris *et al*., 1997). In addition, the presence of terrigneous quartz grains and low organism diversity, refer and support an intertidal zone environment (Flugel, 1982).

4.3.5 Intrasparite:

The rocks of this submicrofacies are grayish orange, hard, massive and recrystalline. It consists of homogenous sparry calcite cement, embedding intraclasts of different sizes. The carbonate intraclasts consist of partly recrystallized micritic. Few monocrystalline quartz grains of medium to coarse sand size encountered (Plate 2, Fig. 8).

***Interpretation*:**

The occurrence of intraclasts within the sparite facies suggest reworking from the nearby carbonate shoals to the shallow subtidal water where sparry calcite is formed (Wilson, 1975 and Flügel, 1982). This can take place during storm influence on deposition in the shallow subtidal zone (Lee and Kim, 1992). In addition, Mn-oxide patches and nodular nature of the characteristic limestones may refer and support an occasional period of storm activity (Bàdenas and Aurell, 2001).

4.4 Dolostone:

This facies is recorded only in the Upper Member at the studied section (Fig. 2). The dolomite beds fluctuate in thickness between 0.5- 5 m. It is composed of dolomite rhombs (70%), which are mainly subhedral to euhedral crystals and showing iron stained zonation. This microfacies is subdivided into three submicrofacies, as follows:

4.4.1 Porous (Fenestral) dolostone:

The rocks of this submicrofacies are yellowish brown, and very hard. It consists essentially of dolomite rhombs (70-80%), glauconite pellets (15-20%) and few argillaceous materials (5%). Dolomite rhombs range in size from 300-400μm, idiotopic to xenotopic in texture, equigranular and occasionally exhibit inequigranular mosaic texture. Few green to brown colour glauconite pellets are noticed. Unfilled pore spaces (fenestral) are recorded (Plate 2, Fig. 9).

***Interpretation*:**

The fine crystalline dolomites have been interpreted to be a result of penecontempraneous dolomitization of precursor micrite in supratidal flat sediments during regressive phase in upper intertidal to supratidal setting (Warren, 2000; Qing *et al*., 2001). Most dolomite rhombs are rimed by iron oxides indicating precipitation in reducing conditions below the ground water table (Tucker, 1982). Consequently, the fenestral lime–mudstone is a characteristic upper intertidal facies indicator (Shinn, 1983).

4.4.2 Oolitic dolostone:

The rocks of this submicrofacies are grayish orange, hard and thin bedded. It consists of dolomite rhombs (60-70%) and ooids (20-30%) with few quartz grains (3%) and glauconite pellets (2%). Dolomite forms the

groundmass and displays equigranular idiotopic to xenotopic fabric with cloudy centers and iron oxides rimed. They range in diameter from 100- 300µm. Most ooids have micritic nucleus, while the outer cortices are sparitic and show both radial and concentric structure (Plate 3, Fig.1).

***Interpretation*:**

In general, ooids with concentric structures and ooid aggregates indicate deposition in an intertidal zone of highly agitated shallow water conditions (Strasser, 1986). The regressive phase of dolomite formed in upper intertidal to supratidal setting (Warren, 2000).

4.4.3 Sandy intra-biodolostone:

The rocks of this submicrofacies are grayish orange, cross bedded and very hard. It is essentially made up of dolomite (40-50%), ooids (20-30%), intraclasts (15-20%) and 10-15% quartz grains (Plate 3, Fig. 2). The dolomite rhombs are equigranular, cloudy centers and are stained by clear rims of iron oxides. Ooids are various in sizes, single in type and deformed. The microstructures are concentric and micritic ooids. Intraclasts are granular to very coarse sand size grained. It consists of essentially micritic materials, ferruginous matter and quartz grains. It is partially replaced and/or filled with pseudosparite and dolomite rhombs. As well as medium to fine sand grained, monocrystalline, cracked, moderately sorted, subrounded and have normal extinction are scattered and floated in the dolomite ground mass.

***Interpretation*:**

Oolitic limestones were mainly accumulated in shallow shelves around dispersion cratonic blocks during episodes with mild maritime climate (Van Houten and Puruiker, 1984). Cross-bedding and coarse grain-size as well as abundant ooids and intraclasts suggest that the oolitic dolostone was deposited in a mobile sand-shoal environment in a shallow-water setting.

4.5 Sandstone Lithofacies:

This lithofacies is well recorded in both lower and upper members (Fig. 2). The sandstone beds fluctuate in thickness between 2.5- 6 m. It consists of quartz grains, lithic-fragments, glauconite grains and argillaceous matrix, with patches of ferruginous, siliceous, calcareous and gypsiferous cements. This microfacies is subdivided into three submicrofacies, as follows:

4.5.1 Ferruginous Quartz wacke:

The rocks of this sublithofacies are grayish orange to brownish yellow, slightly hard, fine grained, badly bedded with sandy clay interbeds and iron oxide concretion. It is dominated by quartz grains (65%), argillaceous matrix (20%), ferruginous matter (12%) and few glauconite grains (3%). Most quartz grains are medium, fine to very fine sizes, monocrystalline grained, ill sorted, immature and show normal to slightly undulose extinction. The matrix is essentially composed of scattered patches of clay minerals. The ferruginous materials are reddish to brown in colour, cemented and stained the frame work (Plate 3, Fig.3).

Interpretation:

The low maturity of sandstones and the sub-angular to subrounded quartz grains indicate a proximal source and suggests that this facies was developed close to the shore/ beach, where the quartz grains could be supplied either by river or erosion of the coastal area (Pettijohn *el al*., 1987).

4.5.2 Glauconitic wacke:

The rocks of this sublithofacies are yellowish orange, hard, massive, cross bedded, and laminated upward. It is consists of quartz grains (60-70%), lithic-fragments (15-20%), glauconite grains (90-95%) with patches of ferruginous and calcareous cements. Most quartz grains are very coarse to medium, monocrystalline and surrounded to subangular. Few polycrystalline, normal to undulose extinction, poorly sorted, contain clear overgrowths and have high inclusions. Glauconite grains are brown to reddish and show alteration from original chert grains. Partially glauconite recorded as a cement material disseminated between the quartz grains. Lithic-fragments are forming less than 20% of the total rock type. They composed of bioclasts and chert grains. In addition, the clay matrix and ferruginous, calcareous cement materials admixed with each other and form yellow to brown thin laminae, disseminated between quartz grains (Plate 3, Figs. 4and 5).

Interpretation:

The argillaceous cross bedded and poor-moderate sorted nature of this facies is indicative of peritidal environment (supra- intertidal flat) (Shinn, 1983)

4.5.3 Quartz arenite:

The rocks of this sublithofacies are grayish red purple, fine grained, moderately hard, joined, and ferrugineous. It is consists of rich quartz grains (90-95%) with a few patches of ferruginous, siliceous and gypsiferous cementing materials. Quartz grains are coarse to medium, subrounded to rounded, well sorted, mature and monocrystalline. They have normal extinction, clear overgrowths and contain high inclusions indicating igneous rocks provenance (Blatt, 1982). Some quartz grains are cracked pitted and show point, concave - convex and rare sutured contacts (Plate 3, Fig. 6).

Interpretation:

The high maturity of quartz arenite indicates deposition in high energy shallow water at a passive continental margin (Pettijohn *el al*., 1987). Also the sub-rounded to rounded quartz grains seem to exclude prolonged transport. This in turn indicates a more proximal source and suggests that this facies was developed close to the shore/ beach, where the quartz grains could be supplied either by river or erosion of the coastal area.

4.6 Claystone Lithofacies:

4.6.1 Oo-pelclaystone:

This sublithofacies is well recorded in both lower and upper members (Fig. 2). The rocks of this facies are varicolored, slightly hard, highly ferruginated and bedded with gypsum bands. Each bed of this facies attains a thickness of 7.5m. It is composed essentially of argillaceous materials admixed together with calcareous matter and peloids (20-30%) and ooids (10-20%). Peloids are more abundant than ooids; they are well rounded, well sorted and exhibiting micritization. Ooids are deformed, truncated and most of them are coated and stained with ferrugineous materials.

Interpretation:

The occurrence of gypsum filled desiccation cracks in the claystone can be related to arid climate in a supratidal sabkha setting (Bauer *et al*., 2001). The occurrence of bioturbated clay intercalated with lenses of sandstones indicates mixed mud-sand tidal flat deposition (Reineck and singh, 1975). Red green molting and bioturbations in claystone reflect deposition in a supratidal- intertidal flat area (Selley, 1996).

5. Diagenetic Sequence:

5.1 Diagenetic Sequences in Carbonate Sediments:

The nature of diagenetic processes operating in carbonate sediments is predominantly of chemical nature and can be grouped into isochemical (processes rendering sediment into a rock without any drastic chemical change) and allochemical (processes with notable change in chemical composition). In carbonate rocks, diagenetic overprinting has greatly affected the lower and upper limestone members of Risan Aneiza Formation. The diagenetic features, identified and interpreted, are micritie envelopes**,** dissolution of aragonite, cementation, compaction and stylolite formation, fractures, and dolomitization (Table 1A). A detailed account of the sequence of various diagenetic phases and their products depending on time hierarchy is presented here:

Table 1: Paragenetic sequences of Risan Aneiza Formation; A: In carbonate sediments and B: In sandstones.

A

Diagenetic events	Time →
Micritic envelopes	
Dissolution of aragonite	
Cementation	
Mechanical compaction	
Chemical compaction	
Dolomitization	
Incorporation of iron into calcite and dolomite	

B

Diagenetic events	Time →
Compaction	
Silica cementation	
Feldspars dissolution	
Carbonate cementation	
Silica dissolution	
Kaolinite and iron oxide cementation	
Carbonate dissolution and evaporite cementation	

5.1.1 Micritic envelopes:

It is the first diagenetic phase, which takes place in the marine diagenesis of limestones. Micritic envelopes developed as a result of microbial boring of skeletal/nonskeletal grains and serve to protect the outline and morphology of affected grain. These envelopes are commonly found on grains with original aragonitic mineral composition. Aragonite, being metastable among carbonate minerals, is dissolved in the first phase of diagenesis of carbonate sediments and is replaced by micrite, hence the micritic envelopes. The later are found on skeletal and non-skeletal grains in different microfacies of this formation (Plate 1, Figs. 3and 6, Plate 2, Figs. 2and 6).

5.1.2 Dissolution of aragonite:

In the second phase, the aragonite dissolves in the faunal grains having aragonitic mineralogy and is precipitated as sparite (Plate 1, Figs. 1and 6). Sometimes the internal structure of the skeletal grains is totally destroyed and no relict structure is observed at all (Plate 3, Fig.5). However, the outline and morphology of these grains is preserved.

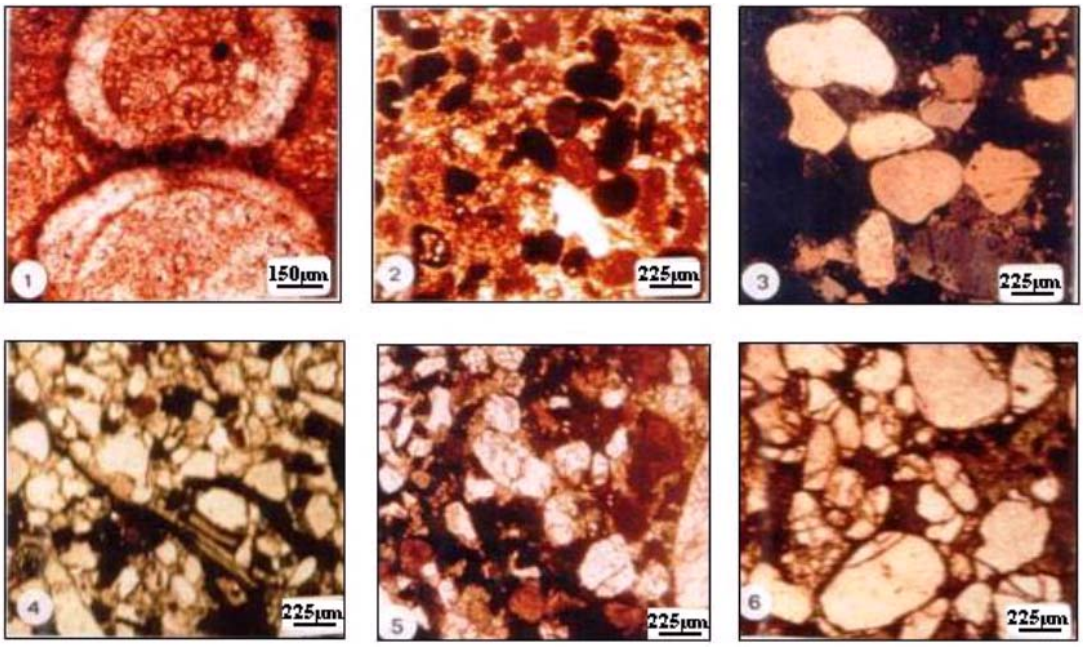

Plate 3: Photomicrograph showing; 1: Large normal ooids, concentric structure and outer cortices are sparitic embedded in dolomite cement. PPL, Bed No. 48, **2**: Ooids and intraclastics from pre-existing sediments set in dolomitic cement. PPL, Bed No. 63, **3:** Ferruginous arenite, well sorted, intensive corrosion of quartz grains cemented with iron oxides. C.N, Bed No. 3, **4:** Glauconitic lithic wacke, rounded medium glauconitic grains with partial intensive corrosion of quartz grains. Note, molluscan lithic fragments, PPL, Bed No. 59, **5**: Glauconitic lithic wacke, corrosion quartz grains by calcareous cement. Notice, recrystallization of skeletal fragments into drusy calcite. PPL, Bed No. 59, **6:** Glauconitic ferruginous quartz wacke, showing quartz grains, grains contact and silica overgrowths. Note, argillaceous material matrix admixed with silica overgrowths. PPL, Bed No, 58.

5.1.3 Cementation:

Cement endows strength and stability to the carbonate microfacies and sediments. The well developed cement, always, resists physical, as well as, chemical compaction and fracturing episodes. Hence, the cementation of carbonate sediments is taken as an important diagenetic process. Early diagenetic cement precipitates as fibrous aragonite, while dog tooth cement (circumgranular equent cement), dolomite cement, drusy mosaic cement and poikilotopic cement precipitate as late diagenetic cements. Intergranular cement is the next phase of carbonate diagenesis. The following cement types have been recorded at different levels and in different microfacies:

The dog tooth cement precipitates as late diagenetic cement. It is circumgranular equent cement (Plate 1, Fig. 8 and Plate 3, Fig. 1).

Circumgranular columnar or prismatic cement (Plate 2. 3) precipitates in the mixed meteoric/marine phreatic environments (Tucker, 1988).

Drusy calcite cement is a pore filling cement. It might be composed of sparry calcite or dolomite. Its crystals are of small size at margins and gets larger towards the centre of pore (Plate 2, Fig. 8). It precipitates in the meteoric phreatic environment (Tucker, 1988).

Poikilotopic cement is elucidated as coarse cement crystals enclose component allochems, which look like specks in crystals mosaic (Plate 2, Fig. 9and Plate 1, Fig. 4). It develops after the phase of pervasive dolomitization and development of intergranular cements and precipitates in phreatic environment, commonly, in burial regime.

5.1.4 Mechanical compaction:

Mechanical compaction of the carbonate sediments is the next diagenetic event. Under this diagenetic process the inter-grain and interstitial space reduces. In case of poorly cemented sediments, the component grains may break due to increased mechanical compaction (Plate 1, Fig 3). The presence of different types of fractures, veins and broken allochems display the imprints of both tectonic stresses and overburden pressure pre-and-post cementation phases. Fractures are commonly found at various horizons in the measured section. Different phases of fracturing, sometimes along with stylolitization, filled with one or more episodes of calcite/ferroan calcite and dolomite/ferroan dolomite have been identified here (Plate 1, Fig.4and Plate 2, Figs. 3 and 7).

5.1.5 Chemical compaction:

The signatures of chemical compaction and stylolite formation have been recognized as close packing (Plate 1, Fig.2; Plate 2, Fig.7) and deformed morphology of component grains in various microfacies (Plate 1, Fig. 3). Point (Plate 1, Figs. 3and7), planner (Plate 1& 3) and sutured grain contacts (Plate 2, Fig.7) and inter-grain embayments (Plate 2, Figs 3) are produced as a result of compaction. Increased tectonic stresses and/or thousands meters overburden pressure produce ultimately pressure solution seams, known as microstylolites in thin section study (Plate 1, Figs. 3and4; Plate 2, Fig. 3). The features are in conformity with the action of pronounced tectonic stresses, which is also confirmed by the presence of folding and faulting, from small scale to regional scale, in the area hosting studied formation. The most of the microstylolites are found cross cutting the fractures and thus postdate the fracturing of that microfacies (Plate 1, Fig. 4; Plate 2, Fig. 3).

5.1.6 Dolomitization:

The texture preserving dolomitization is the next phase of the diagenetic history of limestones, in which only selective dolomitization of matrix took place. The diagenetic process of dolomitization results in the formation of dolomite of secondary nature. In the investigated rooks, the dolomitization is relatively fairly extensive and has developed at its different horizons. Dolomite is present as pore filling cement (Plate 1, Fig. 9; Plate 2, Fig. 9). The following types of dolomitization have been observed in the studied section:

Matrix selective dolomitization is restricted to the matrix that attacks the matrix and destroys it (Plate 3, Fig. 2).

Pervasive dolomitization is an extensive dolomitization process in limestones, in which the dolomitization is not texture selective and attacks the fabric of rock, hence whole of the rock gets dolomitized with the passage of time (Plate 2, Fig.9).

Microdolomitization is such a type of diagenetic process, in which crystals of dolomite developed in a very small size (Plate 1, Fig. 1).

Zoned dolomitization is indicative of changes in the geochemistry of formation fluids during the growth of dolomite crystals. The noted zoned dolomitization has partially affected the concerned microfacies (Plate 1, Fig.9). It is related to uplift of the basin and/or to the unconformity surface.

5.1.7 Incorporation of iron into calcite and dolomite:

It is the last diagenetic setting in which the leached out iron from various sources gets incorporated into calcite (rendering it into ferroan calcite) and dolomite (rendering it into ferroan dolomite) as per demand of the prevailing environmental conditions. This setting is related with the late stage uplifting and/or unconformity surface. It is the post uplift diagenetic phase. The leached out iron is incorporated in calcite and renders it into ferroan calcite (Plate 1, Fig. 1; Plate 2, Fig. 1). The ferroan dolomite (Plate 1, Figs.1, 7and 9; Plate 3, Fig.2) is formed by the same diagenetic process.

5.2 Diagenetic sequence in sandstones:

The major diagenetic aspects observed in the lower and upper members of Risan Aneiza sandstone are: compaction, silica overgrowth, carbonate cementation, mixture of clay and iron oxides filling, iron oxides cementation and evaporite cementation (Table 1B).

5.2.1 Mechanical and chemical compaction:

Several elements such as packing of the framework grains, fractures and dissolution seams within Risan Aneiza sandstones indicates the presence of mechanical and chemical compaction in different stage of diagenesis. Mechanical compaction includes fracturing of quartz and feldspar grains (Plate 3, Figs.5and 6). Chemical compaction occurred by pressure dissolution both along intergranular contacts and fractures. Long and concave- convex grain contacts are the two main types of contacts (Plate 3, Figs. 3and 6).

5.2.2 Cementation:

Cementation by silica, carbonates, iron was recorded in the studied sandstones resulting in partial or complete filling of pore spaces.

Silica cement commonly occurs as overgrowths on detrital quartz grains (Plate 3, Figs.3and 6). Where calcite and quartz cement coexist, the edge of quartz cement may be irregular or rounded and overlain by calcite cement, indicating that calcite cements postdated quartz overgrowth (Plate 3, Figs. 4and 5). Feldspars dissolution and transformation of clay minerals are the main source of SiO_2 for quartz cement.

Carbonate cement: The early calcite cement occupies most of the pore spaces in approximately 30% of studied sandstone samples, which ceased compaction of these sediments. The late calcite cement is indicated by the presence of calcite as fracture- filling and poikilotopic cement. However the amount of late calcite is less than 2%. Quartz overgrowths are engulfed and corroded by calcite and /or dolomite cement (Plate 3. 4and 5) indicating calcite and dolomite cement postdates silica overgrowths.

Dolomite occurs as rhombic crystals with variable crystal size (<25 - 100μm). Microcrystalline dolomite (<25μm) occurs as pore filling cement. Zoned dolomite (>100μm) occurred as scattered patches of discrete or aggregates or rhombic crystals that tend to fill the remaining open pores after coarse crystalline calcite (Plate 3, Fig. 5). The zoned dolomite engulfs, thus postdates microcrystalline dolomite.

Admixture of clay minerals and iron oxide filling: The loss of the calcite and /or dolomite cement and many unstable detrital grains indicates that acid formation water flowed freely through most of the sandstone. Meteoric water evidently invaded the sandstones after they had been uplifted. Local patches of clay minerals (kaolinite) formed at this time, as well as iron oxide cements, including hematite (Plate 3, Fig. 5). These iron oxides form at the surface or in the oxidized zone of the water table.

Iron oxides: The time of dissolution event can only be dated as pre- Cenomanian (Abdel Wahab, 1998). The dissolved cement in most cases was replaced by gypsum. The Aptian- Albian sandstones were reburied by Cenomanian and younger rocks. By this time, the sandstones had a stable quartz rich mineral composition, so that further solution was minor. During Oligocene – Miocene time, the area was strongly affected by rifting, which involved arching, uplift and faulting, that lead to a younger generation of iron oxides, which post date tectonic fractures (Plate 3, Fig. 6).

Evaporites (Gypsiferous cement): The evaporites that leached by modern meteoric water from nearby outcrops of Miocene and younger marine evaporite-bearing strata, transported in surface and ground water to the topographically low terrain where the Aptian- Albian sandstones crop out, and then precipitated by evaporation of surface water.

6. Geochemical Characteristics:

Eleven trace elements (Cr, Mn, Co, Ni, Cu, Zn, Pb, Rb, Ba, Sr and U) have been qualitatively determined in 19 bulk samples representing the various facies (Table 2). These trace elements except uranium were analyzed by atomic absorption spectrophotometry. The fluorimetric technique was used for the analysis of uranium.

6.1 Correlation coefficient and Cluster analysis:

The correlation coefficient between the analyzed trace elements was computed using SPSS16 (Table 3). Cu and Sr are concentrated in micrite facies, while Mn and Zn are enriched in sparite and microsparite facies (Table 2). Cr, Co, Ni, Rb, Ba, Pb and U are concentrated in claystone facies. There are highly positive correlations between Cr, Ni, Rb and Pb and between Sr, Ba and Pb, (Table, 3A, B), which indicate their derivation from mixed source rock. On the other hand, there are highly negative correlations between Cr, Co and Cu, which reflect their derivation from the terrigneous or mixed (carbonate and siliciclastic) sources. Carbonate facies are highly positively correlated with Sr (Table 3A), which indicate their original concentrations in the skeleton of marine organisms. A relatively high concentration of Cu, Mn and Zn in the carbonate facies reflects non influence of terrigneous sediments.

Based on trace elements variations, particularly the proportions of transition elements resulted in three clusters involving three associations (Fig. 3). Cluster 1, Cu-U associations (8 samples), represents 42% of the total samples and has the highest Cu and U percentage and concentrated mainly in claystone microfacies and not recorded in micrite, sandstone and dolostone microfacies. Cluster 2, Cr-Co-Ni- Mn-Zn-Rb associations (7 samples), represents 37% of the total samples, and is characterized by the highest transitional elements and Rb. This association involves samples from all studied microfacies expect micrite microfacies. Cluster 3, Sr-Ba-Pb associations (4 samples), represents 21% of the total samples and has the highest Sr, Ba and Pb contents. It is concentrated in micrite and microsparite microfacies.

6.2 Geochemical Significance:

The chemistry of trace elements is very useful geochemical indicators and may help to shed light on their depositional environment and source rocks. The content of some trace elements (Mn, Sr and U) are plotted

against sample position in the studied lithostratigraphic section to illustrate the vertical distribution of these trace elements (Fig. 4). The vertical distribution of uranium in the Lower Cretaceous of Gabal Manzour section reflects a general upward weak increases in the content together with increases of Sr. It just shows enrichment in the claystone and underlying phosphatic beds (Fig. 4), which means that the uranium most probably leached from the phosphatic beds and adsorbed on the clay minerals forming the claystone beds. The latter contains remains of plant and gypsum. It can be interpreted to the gradual shallow of the, marine conditions upward.

The concentrations of the trace elements in the studied Lower Cretaceous microfacies of Gabal Manzour section show some vertical variations (Table 2 and Fig. 5).

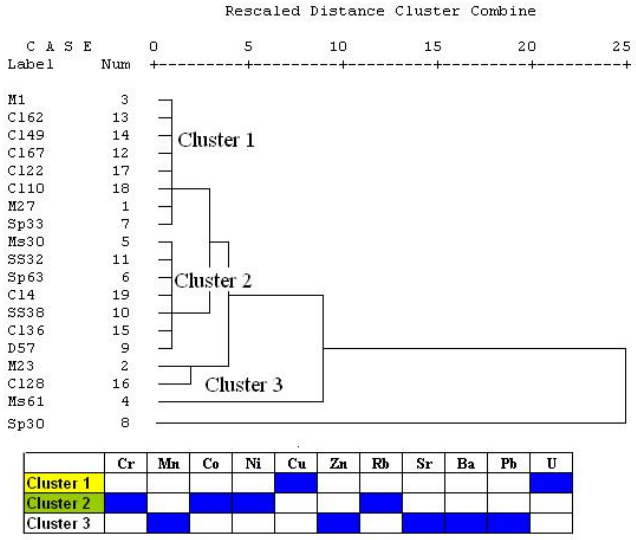

Fig. 3: Cluster analysis of the Lower Cretaceous rocks using trace elements.

Table 2: Chemical analysis data of trace elements (ppm).

Facies		Bed No	Element										
			Cr	Mn	Co	Ni	Cu	Zn	Rb	Sr	Ba	Pb	U
Carbonate microfacies	Micrite	27	5	140	14	4	45	16	2	308	2	16	9
		23	31	162	32	40	22	35	10	820	49	28	3
		1	20	5	5	2	21	89	12	102	10	8	4
		average	15.3	102.3	17	15.3	22.7	46.7	8	410	19.7	17	5
	Microsparite	61	8	1300	20	12	30	50	n.d	225	2	4	1
		30	28	529	12	38	30	34	4	162	4	4	4
		average	18	914	16	25	30	42	2	194	3	5	2.5
	Sparite	63	14	626	16	9	30	30	n.d	120	n.d	n.d	4
		33	63	302	22	34	30	188	28	200	28	44	2
		19	28	1755	69	46	25	1020	2	42	2	5	n.d
		average	35	894	35.7	29.7	28	413	10	121	10	15	2
	Dolostone	57	30	844	41	30	30	66	28	180	1	2	n.d
		average	30	844	41	30	30	66	28	180	1	2	0
Clastic lithofacies	Sandstone	38	25	556	2	11	30	50	2	338	2	n.d	2
		14	19	500	2	9	40	50	2	94	8	n.d	0.1
		average	22	528	2	10	35	50	2	216	5	0	1
	Claystone	67	38	4	4	8	41	90	20	232	12	10	4
		62	17	10	5	45	43	92	8	82	n.d	36	7
		49	19	18	10	34	45	94	10	130	10	n.d	50
		39	156	556	70	79	n.d	76	20	320	n.d	46	2
		28	107	410	11	71	30	31	40	548	60	48	3
		21	33	166	12	14	25	30	6	62	6	2	n.d
		10	44	228	32	46	40	90	10	32	10	10	1
		4	144	604	9	33	25	50	60	130	2	n.d	4
		average	68.8	273.5	19.1	41.3	31	69.1	22	192	12.5	19	7

6.2.1 Uranium:

In the supergene cycle, uranium is removed from sea water by several processes, in which the ability of uranium to form stable complexes with various species may play an important role. Marine limestones generally contain about 2 ppm of uranium; so for discussion of uranium behavior in aqueous solution has stated that

uranium stay in solution if carbonate ions are present. According to Naumov and Mitronova (1969), the decomposition of uranyl carbonate complexes and the simultaneous reduction of uranium proceed more readily with decreasing carbonate ion concentration. In fact, the potential of U^{6+}- U^{4+} couple in the presence of CO_3^{2-} ions is lower than that in carbonate free waters that is, more reducing conditions are required to remove uranium from carbonate-rich water in comparison with waters low in carbonate.

Table 3: Correlation coefficient of chemical composition of carbonate (A) and clastic (B) sediments.

A:

	Cr	Mn	Co	Ni	Cu	Zn	Rb	Sr	Ba	Pb	U
Cr	1										
Mn	-0.119	1									
Co	0.225	0.730*	1								
Ni	0.638*	0.369	0.684*	1							
Cu	-0.330	-0.111	-0.235	-0.358	1						
Zn	0.193	0.697*	0.827**	0.513	-0.264	1					
Rb	0.752**	-0.275	0.086	0.269	-0.161	-0.133	1				
Sr	0.055	-0.411	-0.036	0.214	-0.108	-0.354	0.038	1			
Ba	0.537	-0.458	0.005	0.392	-0.412	-0.148	0.338	0.818**	1		
Pb	0.705*	-0.465	-0.072	0.266	0.006	-0.080	0.499	0.479	0.782**	1	
U	-0.421	-0.669	-0.633	-0.561	0.618*	-0.458	-0.359	0.178	-0.040	0.107	1

B:

	Cr	Mn	Co	Ni	Cu	Zn	Rb	Sr	Ba	Pb	U
Cr	1										
Mn	0.610*	1									
Co	0.613*	0.270	1								
Ni	0.662*	0.188	0.703*	1							
Cu	-0.786	-0.622	-0.750	-0.497	1						
Zn	-0.240	-0.572	0.217	0.104	0.344	1					
Rb	0.784**	0.365	0.058	0.376	-0.298	-0.255	1				
Sr	0.444	0.379	0.130	0.440	-0.380	-0.363	0.338	1			
Ba	0.182	0.022	-0.146	0.379	0.099	-0.393	0.354	0.681*	1		
Pb	0.477	0.042	0.510	0.849**	-0.413	0.050	0.218	0.574	0.450	1	
U	-0.253	-0.451	-0.122	0.018	0.369	0.447	-0.098	-0.129	-0.022	-0.209	1

* Correlation is significant at the 0.05 level, ** Correlation is significant at the 0.01 level

In the studied sediments, the highest value of uranium in carbonate facies belongs to micrite and microsparite (average = 5 ppm), while it decreases in sparite microfacies. This means that uranium decreases with diagenesis. This may be due to its breakdown during second precipitation. The uranium is not detected in dolostone microfacies most probably there is no substitution between U^{2+} and Mg^{2+} (0.8A^o). The values agree to some extent with the international values (e.g Adams *et al*., 1959). The uranium content in carbonate sediments is expected to be controlled more by biological factors than by pure chemical precipitation.

In the clastic sediments, the high uranium content occurs in claystone beds containing plant remains and gypsum (50 ppm, av. = 9 ppm), because of they release uranyl complex by SO_4. The relationship between uranium and sulphate minerals favours role evaporation process as most acceptable explanation for this phenomenon, which can be clearly observed in the field by the presence of gypsum in the mineralogical composition of bed rock. The evaporation process is confirmed to the alkaline depositional environment with pH values ranging from 7.9 to 8.6. Trapping of the uraniferous solution within suitable geological environment, structural and lithological sites represented in our study by clastic facies especially claystone beds. Katayma *et al*., (1974) mentioned that clay minerals may represent an important stage in uranium concentration. This was also confirmed by Gauther's (1964) experimental work on adsorption or co-precipitation of uranium by different types of clay minerals.

In the present work, it was found that the analyzed uranium shows positive relation with some trace elements; Ni and Cu (Table 3), and a weak with Zn (Fig. 6) due to their adsorption on clay minerals.

6.2.2 Strontium and Manganese:

The analyzed sediments are markedly depleted in Sr especially in the carbonate microfacies (Sr = 239 - 610 ppm after Wedepohl, 1991), most probably due to extensive post depositional processes. The content of Mn varies from one microfacies to another. It seems to be enriched in carbonate microfacies especially in sparite submicrofacies where, it reaches 1755 ppm. The Sr concentration decreases with increasing Mn values. The concentrations of Sr and Mn in calcite are largely related to the distribution coefficient, water system, flow condition and chemistry of entering water (Pingitore, 1978; Brand and Veizer, 1980). As the distribution coefficient of Sr ($K^{Sr}_{Calcite}$= 0.14, Kinsman, 1969) and Mn ($K^{Mn}_{Calcite}$ = 15; Pingitore, 1978) in calcite differs markedly, the calcite precipitation during diagenesis will have lower Sr and higher Mn concentration than in the

precursor calcite, like the decrease of Sr and increase of Mn concentration. In a closed aqueous system, where there is no large scale movement of ions, the calcite precipitating, with no external source of Sr and Mn, should contain almost similar total amount of Sr and Mn as its calcite precursors. As the observed values of Sr are lower and Mn are much higher than in the original sediments, the aqueous system was not closed during the diagenesis of limestone. In open aqueous system water, there is a large scale movement of ions, the calcite precipitating with no external source of Sr and Mn could have lower Sr and higher Mn concentration than in precursor calcite. The high Mn concentration in limestone is due to accumulation of Mn released from internal dissolution of $CaCO_3$ precursors (autoenrichment) or from an external supply of Mn in liquid (alloenrichment) entering into system. As the initial dissolution of metastable aragonite and Mg- calcite or calcite (<50 ppm Mn) and reconcentration of calcite with little external Mn results in moderate increase of Mn in vedose and phreatic diagenesis, subsequent dissolution of large volumes of calcite is needed (Meyers, 1974 and Pingitore, 1978) to account for high Mn concentration up to 20-25,000 ppm. The highest Mn concentration and the marked clear antipathetic relationship with Sr indicates that the source of Mn was both external and internal.

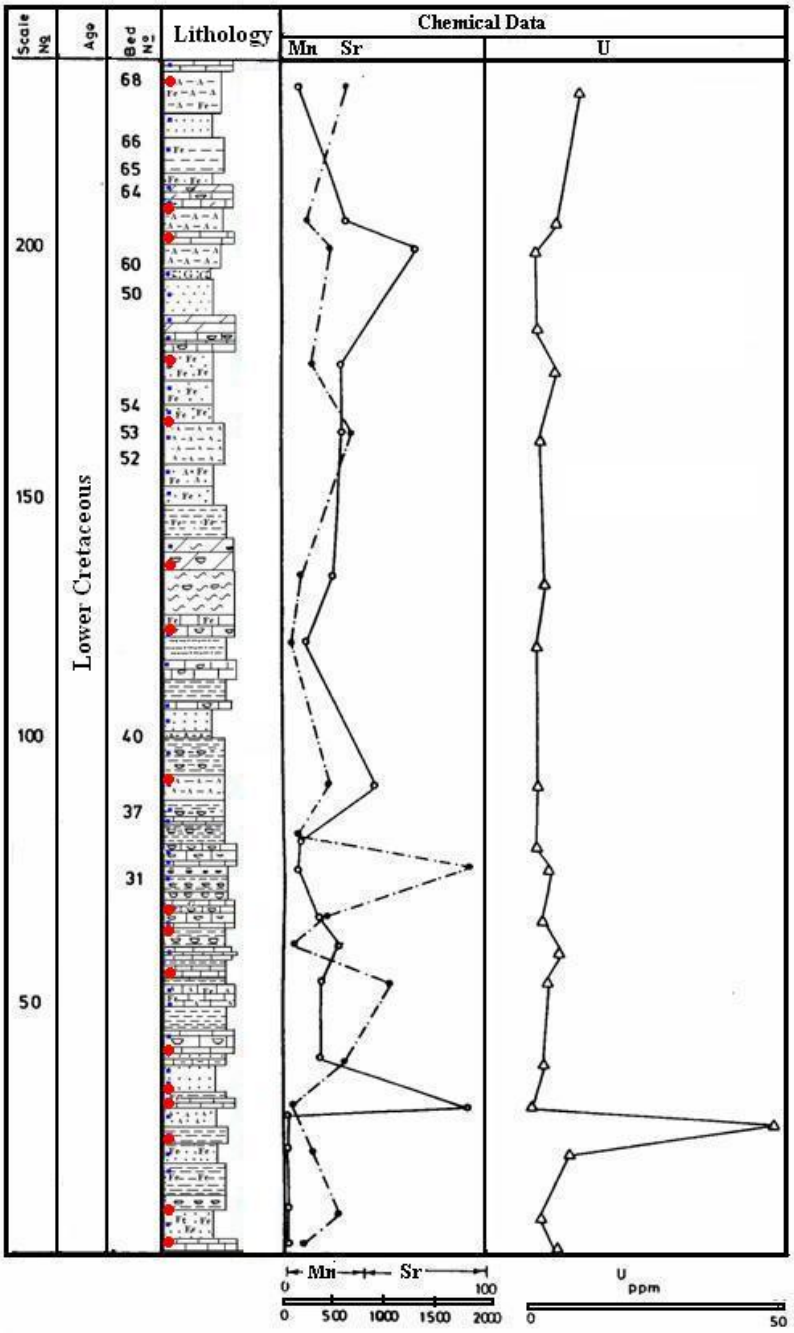

Fig. 4: Vertical distribution of Mn, Sr and U concentration in studied rocks.

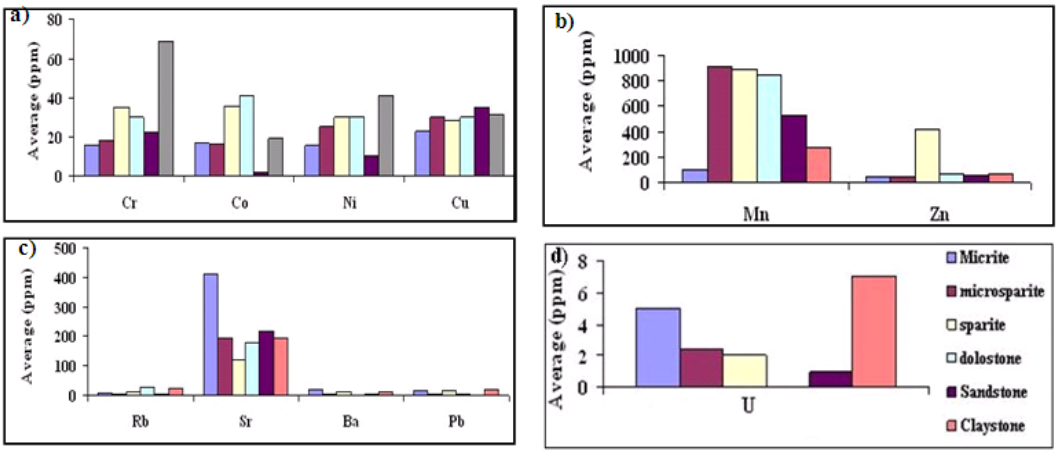

Fig. 5: Distribution of trace elements in microfacies of Gabal Manzour rocks.
a-Transitional elements distribution b- Mn and Zn distribution
c- Rb, Sr, Ba and Pb distribution d- U distribution

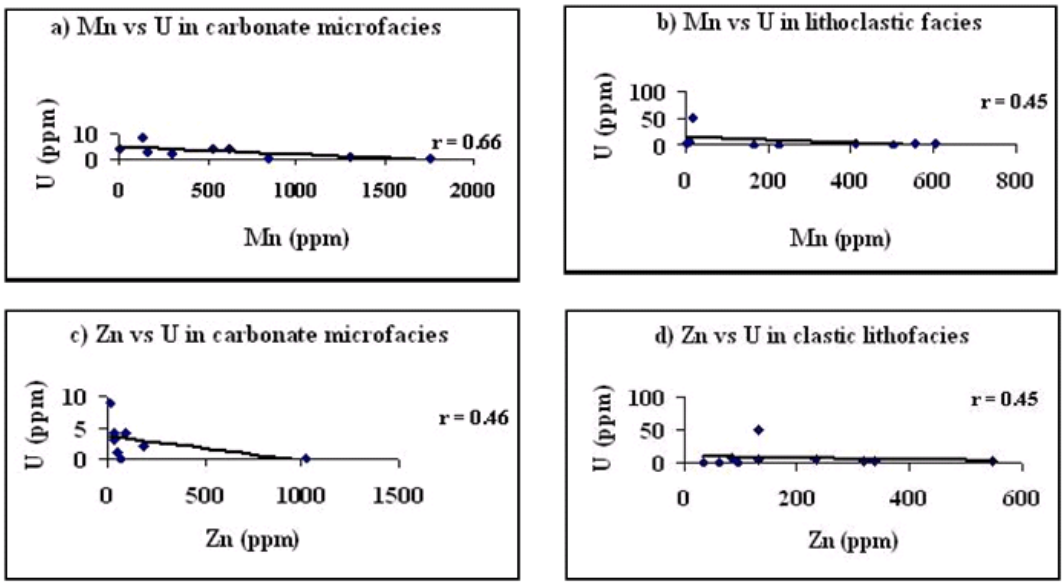

Fig. 6: Relation between U and some trace elements in microfacies of Gabal Manzour rocks.

6.2.3 Rubidium, Barium and Lead:

The relative distribution of Rb in the studied sediments is controlled by lithology, where Rb reaches its highest magnitude (60 ppm) in the clastic microfacies especially claystone submicrofacies and its lowest values in the carbonate microfacies. Rb is typical diad for K in the clay and silicate minerals.

Similar to Sr, the studied sediments are exceptionally depleted in Ba, with ranges from 1 - 49 ppm in carbonate microfacies and from n.d - 60 ppm in clastic lithofacies. There is positive correlation between Ba and Pb in carbonate microfacies (r= 0.78) and weak correlation in the clastic lithofacies (r = 0.45), This can be interpreted as due to geochemical affinity of Ba to be associated with many Pb-Zn sulphide ore as noted elsewhere by Levinson (1980).

The Pb concentration in the carbonate microfacies ranges between (n.d - 44 ppm), where its average concentration in micrite microfacies (15 ppm), microsparite (4 ppm), sparite (16.3 ppm) and dolostone microfacies (2 ppm). This is due to that Pb^{2+} (1.32A^{o}) has affinity substitution to Ca^{2+} (1.06 A^{o}) in calcite.

Lead is not detected in sandstone lithofacies while the average concentration of lead is 19 ppm in the claystones beds, which most probably due to their adsorption on the clay minerals.

6.2.4 Transition elements:

Geochemical characteristics of Cr, Co, Ni and Zn in the bulk sediments; carbonate and clastic facies are controlled mainly by textural composition of the beds. In the carbonate microfacies, the analyzed transitional elements Cr, Mn, Ni and Zn show intimate correlation with each other. Cobalt gives a moderate positive correlation with Zn, Ni and Mn (r = 0.83, 0.68 and 0.73, respectively), Cr with Ni (r = 0.64) and Mn with Zn (r = 0.70).

The clastic microfacies, with a few marked exceptions, the analyzed transitional elements do not show intimate correlation with each other, most probably due to their fractionation among varies mineral phases. Chromium shows a positive correlation coefficient with Mn (r = 0.49), Co (r = 0.61), Ni (r = 0.63) and a negative correlation with Cu (r = -0.79). Cobalt shows a positive correlation with Ni (r = 0.64) while it shows a negative correlation with Cu (r =- 0.75). Ni shows a positive correlation with Pb (r = 0.84), while Mn show a negative correlation with Zn (r = -0.64). The claystones register higher concentration of trace elements than that in the sandstones dominant sediments.

The granulometric analysis studies also re-affirmed the role of particle size in enriching the trace elements (Padomlal *et al*., 1997). The enrichment factors of Cr, Co, Ni and Zn in claystones compared to that in sandstone, are 3.2, 9.5, 4.1 and 1.2 times respectively.

The investigated clastic facies especially claystones are significantly enriched in Cr, Co and Ni compared to the average shales of Wedepohl (1991). Generally, detrital Cr minerals present are of significant important, it probably entered the basin of deposition in lattice position of clay minerals. Frohlich (1960) postulated that the bulk of Cr present in sediments is associated with clays especially illite. The association of Cr, Co and Ni may interpret in terms of partitioning of these elements by cation exchange process in smectite (Jarvis and Higgs, 1987).

Copper, is enriched in the studied carbonate microfacies with an average = 29 ppm, compared with the average of Krauskopf (1979), 4 ppm. The marine carbonate sediments are scavenger of Cu contained in seawater. In the clastic lithofacies, its average content 32 ppm, where it is most probably adsorbed on the clay minerals.

Uranium and other elements entered the Lower Cretaceous sediments may be due to weathering crust or sea water. The distribution trends are clearly related to the environment of sedimentation and their dynamics. The data indicate how the facies affect the features of the rocks

Conclusion:

1. The study deals with the Aptian- Albian sediments encompassed in Gabal Manzour, Maghara area. The study revealed six microfacies (micrite, microsparite, sparite, dolomite, sandstone and claystone) with twenty submicrofacies. The variation of these microfacies can presumably be interpreted as consistent change in the depositional environment. The microfacies analysis indicates transition from interior ramp environments (i.e., lagoon, backshoal, and shoal); intertidal and low-energy subtidal facies interfingers with a few storm-influenced deposits occur. The main factors controlling facies deposition were eustatic sea-level fluctuations and autochthonous carbonate productivity and siliciclastic supply. Diagenetic process affected on studied carbonate rocks are micritic envelopes**,** dissolution of aragonite, cementation, compaction and stylolite formation, fractures, and dolomitization ,while on sandstone one are: compaction, silica overgrowth, carbonate cementation, mixture of clay and iron oxides filling, iron oxides cementation and evaporite cementation.
2. Evidence of diagenetic alteration: petrographic examination of Gabal Manzour sedimentary rocks reveals that original lime (or micrite) from the carbonate facies has been recrystallized to microsparite and sparite. This textural change clearly reflects diagenetic alteration. Microsparite and sparite beds with high Mn concentrations are characterized by low Sr concentrations. These elemental variations are also clearly the results of diagenesis because diagenetic alteration commonly results in Sr depletion and Mn enrichment (Brand and Veizer, 1980).
3. In the studied section; some sediments show that the Zn content is seriously depleted, suggesting preferential mobilization of Zn upon weathering.
4. The low content of Mn in some beds indicates either oxidizing fluids or no significant sources in this element in the diagenetic system. In contrast, high Mn must indicates reducing pore water and allochonous sources of this element. Allochonous source in turn indicates a wide spread fluid circulation system and fluid-rock interaction with underlying or adjacent non-carbonate rocks.
5. According to the obtained results the uranium concentration ranges from 2 to 9 ppm in the carbonate facies and from 2 to 50 ppm in the clastic facies of Gabal Manzour sediments. This significant oscillation is most probably influenced by facies type, adsorption and oxidation - reduction process.

6. The correlation coefficient between the analyzed trace elements and varies microfacies show that Cu and Sr are concentrated in micrite facies, while Mn and Zn are enriched in sparite and microsparite facies. Cr, Co, Ni, Rb, Ba, Pb and U are concentrated in claystone facies.
7. The highly positive correlations between Cr, Ni, Rb and Pb and between Sr, Ba and Pb indicate their derivation may be from mixed source rock, while highly negative correlations between Cr, Co and Cu reflect their derivation from the terrigneous sources. As well as carbonate facies are highly positively correlated with Sr indicate their original concentrations in the skeleton of marine organisms. A relatively high concentration of Cu, Mn and Zn in the carbonate facies reflects non influence of terrigneous sediments.
8. Based on trace elements variations; there are three clusters involving three associations namely; Cluster 1, Cu-U associations (in claystone microfacies and not recorded in micrite), Cluster 2, Cr-Co-Ni- Mn-Zn-Rb associations (all types of microfacies except micrite one) and Cluster 3, Sr-Ba-Pb associations(in micrite and microsparite microfacies).

REFERENCES

Aal, A.A. and J.J. Lelek, 1994. Structural development of the northern Sinai, Egypt and its implication on the hydrocarbon prospectivity of the Mesozoic. GEO 94, the Middle East Geosciences Conference Bahrain, I: 15 -30.

Abdel Wahab, A., 1998. Diagenetic history of Cambrian quartz arenites, Ras Dib – Zeit Bay area, Gulf of Suez, Eastern Desert, Egypt. Sedimentary Geology, pp: 121-140.

Aboul Ela, N.M., G.I. Abdel Gawad and M.F. Ali, 1991. Albian fauna of Gabal Manzour, Maghara area, north Sinai, Egypt, Journal of African Earth Sciences, 13(2): 201-220.

Abu El-Hassan, M. and H.A. Wanas, 2005. Dolomitization of the Cenomanian–Turonian carbonate rocks along the western side of the Gulf of Suez: implication to sea level oscillations. Bull. Fac. Sci. Alex. Univ. Egypt 43: 245-270.

Abu-Zied, R.H., 2007. Palaeoenvironmental significance of Early Cretaceous foraminifera from northern Sinai, Egypt, Cretaceous Research, 28: 765-784.

Adams, J.A.S., J.K. Osmand and J.J.W. Rogers, 1959. The geochemistry of thorium and uranium. In Phys. Chem. Earth, 3: 298-348.

Al-Far, D.M., 1966. Geology and coal deposits of Gebel Maghara, north Sinai. Geological Survey Egypt, Paper, 37-59.

Aly, M.F., 1988. Stratigraphical and paleontolgical studies of the Lower Cretaceous in Maghara area (Gabal Manzour), North Sinai, Egypt. unpub. M Sc Thesis, Cairo univ., Cairo, pp: 203.

Ayyad, M.H., M. Darwish and A. Sehim, 1998. Introducing a new structural model for North Sinai with its significance to petroleum exploration. Proc. Egyptian Petroleum Corporation Exploration Seminar Cairo, Egypt, 14(1): 101-117.

Bachmann, M., M.A.A. Bassiouni and J. Kuss, 2003. Timing of mid-Cretaceous carbonate platform depositional cycles, northern Sinai, Egypt. Palaeogeography, Palaeoclimatology, Palaeoecology, 200: 131-162.

Bàdenas, B., M. Aurell, 2001. Proximal–distal facies relationships and sedimentary processes in a storm dominated carbonate ramp, Iberian Ranges, Spain. Sedimentary Geology, 139: 319-340.

Bartov, Y., G. Steinitz, M. Ayal and Y. Ayal, 1980. Sinistral movement along the Gulf of Aqaba: its age and relation to the opening of the Red Sea. Nature, 285: 220-222.

Bauer, J., A.M. Marzouk, T. Steuber and J. Kuss, 2001. Lithostratigraphy and biostratigraphy of the Cenomanian–Santonian strata of Sinai, Egypt. Cretaceous Research, 22: 497-526.

Blatt, H., 1982. Sedimentary petrology, Freeman and Co., San Francisco.

Brand, U. and J. Veizer, 1980. Chemical diagenesis of a multi-component carbonate system, 1. Trace elements. J. Sediment. Petrol., 50: 1219-1236.

Carozzi, A.V., 1960. Microscopic sedimentary petrology. Wiley, New York, 485.

Dunham, R.J., 1962. Classification of carbonate rocks according to depositional textures. In: Ham, W.E. (Ed.), Classification of Carbonate Rocks, vol. 1. American Association Petroleum Geologists Memoir, pp: 108-121.

El-Araby, A., 1999. Facies analysis and sequence stratigraphy of the Late Aptian–Albian Risan Aneiza Formation in northern Sinai, Egypt. Egyptian Journal Geology, 3(2): 151-180.

El-Azabi, M.H. and A. El-Araby, 2005. Depositional facies, environments and sequence stratigraphic interpretation of the Middle Triassic–Lower Cretaceous (pre-Late Albian) succession in Arif El-Naga anticline, northeast Sinai, Egypt. Journal of African Earth Sciences, 41: 119-143.

El Sheikh, H.A. and S.M. Aly, 1994. Biostratigraphic study on the Jurassic- Early Cretaceous rocks in some exploratory wells in north Sinai, Egypt. Egyptian J., Geol., 38-2: 507-524.

Flügel, E., 1982. Microfacies Analysis of Limestone. Springer-Verlag, Berlin, pp: 633.

Frohlich, F., 1960. Beitrang zur Geochemie des chroms: Geochim Cosmochim Acta, 20: 215-240.

Gauther's, M., 1964. Contribution a' la geochemie de l'uranium des roches sedimentaires et en particulier des schistes carboniteres. Bull. Serv., Cart Geol. Alsace., 14: 179.

Hamama, H., 2010. Barremian and Aptian Mollusca of Gabal Mistan and Gabal Um Mitmani, Al-Maghara Area, Northern Sinai, Egypt, Journal of American Science, 6(12): 1702-1714.

Hamza, F.H., A.A. Ismail and M.A. El-Saadany, 1994. Biostratigraphy and paleoecology of some Cretaceous exposures in northern Sinai, Egypt. Egyptian General Petroleum Corporation, 12 Petroleum Exploration and Production Conf., Cairo, pp: 482-495.

Harris, M.K., A.A. Thayer and M.A. Amidon, 1997. Sedimentology and depositional environments of Middle Eocene terrigneous-carbonate strata, southeastern Atlantic coastal plain. Sedimentary Geology, 108: 141-161.

Hassaan, M.M., N.A. Abdel Hafez, A.A. Ahmed, A.A. Dardir and N.A. Arain, 1990. Geological and geochemical studies on the Safa and Masajid Formations and associated coal seam, Risan Aneiza area, northern Sinai, Egypt. Geol. of the Arab world, Cairo Univ., pp: 151-169.

Hassaan, M.M., N.A. Abdel Hafez, A.A. Dardir and N.A. Arain, 1992. Geologic studies in the Cretaceous sedimentary rocks in Risan Aneiza- Gabel Al Amrar area northern Sinai, Egypt. Geol. of the Arab world, Cairo Univ., pp: 353-365.

Hegab, O.A., H. Hamama and N.A. Atia, 1989. Stratigraphy, facies and environment of the Lower Cretaceous of Gabel Um Mitmana, Maghara area, north Sinai,.Proc. 2nd, Conf. Geol. Sinai Develop. Ismailia, pp: 110-120.

Hewaidy, A.A. and A.M. Morsi, 2001. Lower Cretaceous (Aptian-Albian) foraminifera and ostracoda from northern Sinai, Egypt. Egyptian Journal of Paleontology, 1: 229-252.

Hottinger, L., 1997. Shallow benthonic foraminiferal assemblages as signals for depth of their deposition and their limitations. Bull. Geol. Soc. France, 168: 491-505.

Ibrahium, A.M., 1992. Microfacies and diagenetic studies on the Lower Cretaceous rocks of Gabel Lagama area, North Sinai, Egypt. Proceed 8th Symp. Phaner. Develop. Egypt, pp: 1-16.

Issawi, B., M. El-Hinnawi, M. Francis and A. Mazhar, 1999. The Phanerozoic Geology of Egypt: A Geodynamic Approach. Egyptian Geol. Sur., v. 76, Special Publications, pp: 462.

Jarvis, I. and N. Higgs, 1987. Trace element mobility during early diagenesis in distal turbidities. Late Quaternary of Maderita Abyssal plain. N. Atlantic. In: P.P.E. Weaver and Thomson (Eds), Geology and Geochemistry of abyssal plains, Geol. Soc. London, Sp. Publ., 31: 179-213.

Katayma, N., K. Kullur and S. Hirono, 1974. Genesis of uranium deposits of the Tono Mine, Japan. Procc. Symp. Formation of uranium deposits, Athens, IAEA, Vienna, pp: 437-425.

Khalifa, M.A., 1996. Depositional cycles in relation to Sea level changes, Case studies from Egypt. J. Geol., 40(1): 141-171.

Kinsman, D.J.J., 1969. Interpretation of Sr^{2+} concentrations in carbonate minerals and rocks. J. Sediment. Petrol., 39: 486-508.

Krauskopf, K.B., 1979. Introduction to geochemistry (2nd ed): New York, McGraw Hill, pp: 617.

Kuss, J., M. Bachmann, 1996. Cretaceous palaeogeography of the Sinai Peninsula and neighbouring areas. Compte Rendu de l Academic des Sciences de Paris 322, serie IIa, pp: 915-933.

Lee, Y.I. and J.C. Kim, 1992. Storm-influenced siliciclastic and carbonate deposits. The lower Ordovician Dumugol Formation, South Korea. Sedimentology, 39: 951-969.

Levinson, A.A., 1980. Introduction to exploration geochemistry, Calger, Canada, Applied Publishing Ltd., pp: 601.

McRae, S.G., 1972. Glauconite. Earth Science Review, 8: 397-440.

Meyers, W.J., 1974. Carbonate cement stratigraphy of the lake Valley Formation (Mississippian) Sacramento Mountains, New Mexico. J. Sediment. Petrol., 44: 837-861.

Naumov, G.B. and O.F. Mitronova, 1969. Migration of uranium in hydrothermal carbonate solution (according to physicochemical date): In problems of geochemistry Khitarov N.I. ed. (Jerusalem; Israel programe for Scientific Translations), pp: 166-75.

Padomlal, D., K. Maya and P. Seralathan, 1997. Geochemistry of Cu, Co, Ni, Zn, Cd and Cr in the surficial sediments of a Tropical Estuary, Southwest Coast of India-A granulomeritic Approch. Environmental Geology, 31(1-2): 85-93.

Pettijohn, F.J., 1975. Sedimentary rocks 3rd ed., Horper and Row., New York, pp: 286.

Pettijhon, F.J., P.E. Potter and R. Siever, 1987. Sand and Sandstone. Springer-Verlag, New York, 553.

Pittet, P., A. Strasser and C. Dupraz, 1995. Paleoecology, palaeoclimatology and cyclostratigraphy of shallow-water carbonate siliciclastic transition the Oxfordian of the Swiss Jura. In: 16th IAS Regional Meeting of Sedimentology, Field Trip, Book, 23: 225-254.

Philip, G.N.M., M.M. Abu El, G. Abd El Gawad and M.F. Aly, 1988. Facies and Paleaecology of the Albian rocks of Gabel Manzour, Maghara area, north Sinai, Egypt, Egyptian J. Geol., 32(1-2): 173-197.

Pingitore, N.E., 1978. The behavior of Zn^{2+} and Mn^{2+} during carbonate diagenesis: theory and application. J. Sediment. Petrol., 48: 799-814.

Qing, H., D.W. Bosence and E.P. Rose, 2001. Dolomitization by penesaline sea water in Early Jurassic peritidal platform carbonates, Gibraltar, western Mediterranean. Sedimentology, 48: 153-163.

Reineck, H. and I. Singh, 1975. Depositional Sedimentary Environments. Springer- Verlag, Berlin, Heildberg, New York, pp: 618.

Selley, R., 1996. Ancient Sedimentary Environments and Their Subsurface Diagnosis. Chapman Hall, London, pp: 300.

Shinn, E.A., 1983. Tidal flat environment. In: Scholle, P.A., Bebout, D.G. and Moore, C.H. (Eds.), Carbonate Depositional Environments, v. 33, American Association Petroleum Geologists Mem, pp: 173-210.

Smith, A.G., 1971. Alpine deformation and the oceanic areas of the Tethys, Mediterranean and Atlantic. Geological Society of America, Bull., 82: 2039-2070.

Strasser, A., 1986. Ooides in Purbeck limestones (lowermost Cretaceous) of the Swiss and French J. Sedimentology, 33: 711-727.

Tucker, M., 1988. "Techniques in Sedimentology", Blackwell Scientific Publications, Oxford, London, pp: 394.

Tucker, M. and V.P. Wright, 1990. Carbonate Sedimentology. Blackwell Scientific Publications, Oxford, pp: 482.

Van Houten, F. and M. Purucker, 1984. Glauconitic peloids and chamositic Ooloids N favorable factors, constraints, and problems, Earth Science Reviews, 20: 211-250.

Wanas, H.A., 2008. Cenomanian rocks in the Sinai Peninsula, Northeast Egypt: Facies analysis and sequence stratigraphy. Journal of African Earth Sciences, 52: 125-138.

Warren, J., 2000. Dolomite: occurrence, evolution and economically important association. Earth Science Review, 52: 1-81.

Wedepohl, K.H., 1991. The composition of the upper earth's crust and natural resources: In E., Merian (ed.). Metals and their compounds in the environment. New York, pp: 33-39.

Wilson, J.L., 1975. Carbonate Facies in Geological History. Springer-Verlag, Berlin, pp: 471.